## 5.6. Barrow, Alaska (8/28/98 – 11/4/99)

The 1998-99 season at Barrow is defined as the time between the site visits 8/19/98 – 8/27/98 and 11/5/99 – 11/9/99. The season opening and closing calibrations were performed on 8/26/98 – 8/27/98 and 11/5/99, respectively. Volume 8 solar data comprises the period 8/28/98 – 11/4/99. During this time, the system operated normally and the responsivity remained stable to within ±2%. About 98% of the scheduled data scans are part of the published dataset; less than 0.5% of all scans were lost because of technical problems.

### 5.6.1. Irradiance Calibration

The site irradiance standards for the 1998-99 Barrow season were the lamps 200W009, M-762, and M-699. As with all other sites, lamp M-874 was the traveling standard, which was used during season opening and closing calibrations. The lamp has two calibrations from Optronic Laboratories, one from August 1995 and one from September 1998. The calibration from 1998 was used for season opening as well as closing calibrations of the Barrow spectroradiometer.

All three site standards 200W009, M-762, and M-699 had been re-calibrated at Optronics Laboratories in September 1998, before they were used in the Barrow Volume 8 season.

Figure 5.6.1 shows a comparison of all lamps at the beginning of the season (days 8/26/98 and 8/27/98). All site standards agree on the ±1.5% level with M-874. The good agreement can be expected because of their just-prior calibration at Optronic Laboratories. Figure 5.6.2 shows a similar comparison of all lamps for the end of the season (day 11/5/99). The agreement is also on the ±1.5% level, confirming that the lamps did drift less than 1.5% during the season. This gives confidence in the solar data recorded in Barrow during the 1998-99 season.

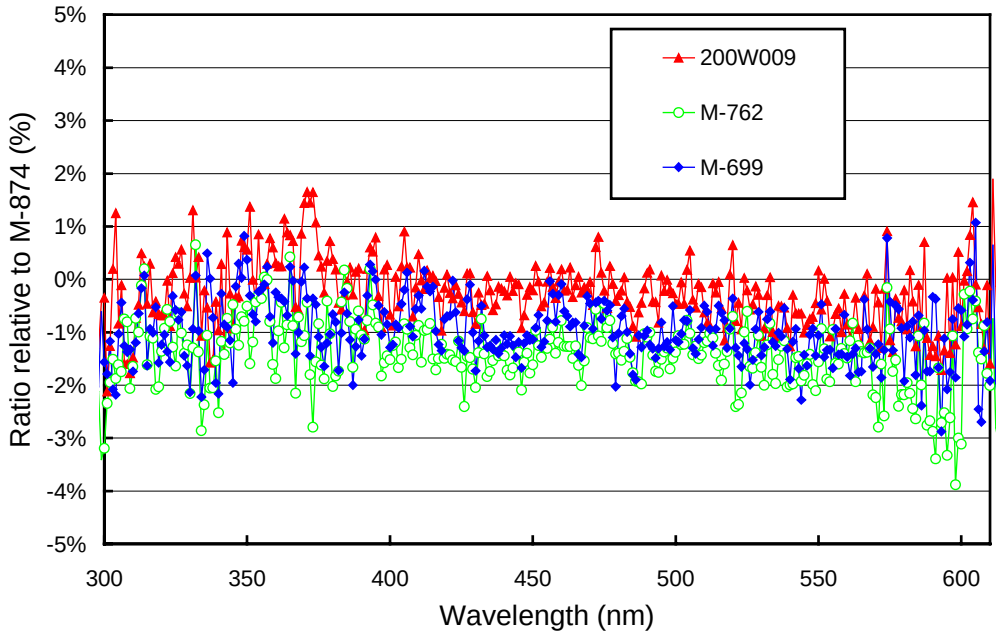


**Figure 5.6.1.** *Comparison of Barrow lamps 200W009, M-762, and M-699 with the BSI traveling standard M-874 at the beginning of the season.*

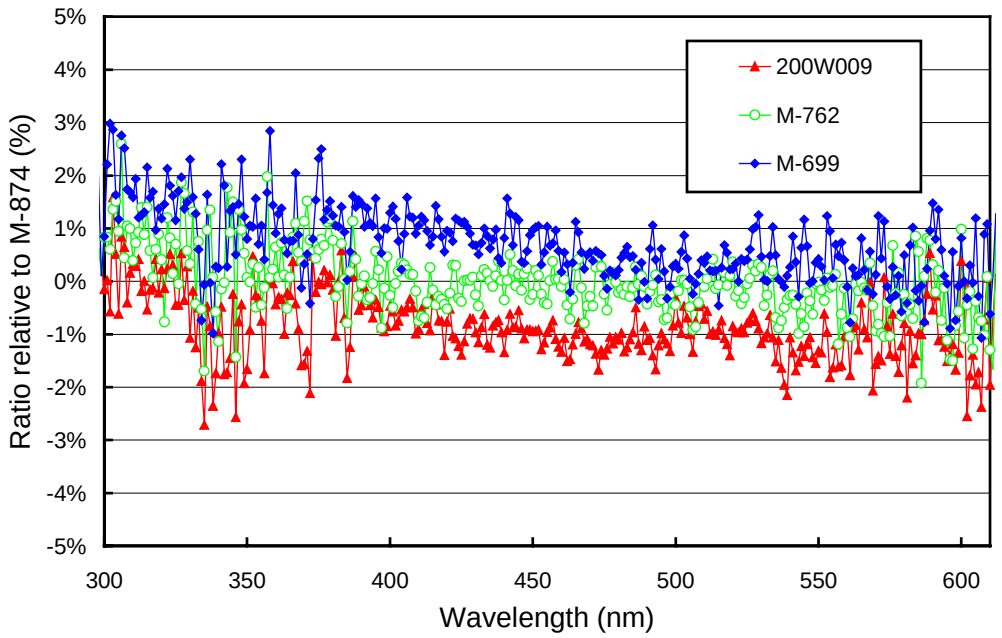


**Figure 5.6.2.** *Comparison of Barrow lamps 200W009, M-762, and M-699 with the BSI traveling standard M-874 at the end of the season.*

### 5.6.2. Instrument Stability

The stability of the spectroradiometer over time is primarily monitored with bi-weekly calibrations utilizing the site irradiance standards and daily response scans of the internal irradiance reference. The stability of the internal lamp is monitored with the TSI sensor, which is independent from possible monochromator and PMT drifts. When TSI measurements indicate that the internal lamp has drifted by more than 2%, a new irradiance is assigned to this lamp, based on the bi-weekly absolute calibrations (see Section 4.2.1.2). By logging the PMT currents at several wavelengths during response scans, changes in the instrument responsivity can be detected.

Figure 5.6.3 shows the changes in TSI readings and PMT currents at 300 and 400 nm, derived from the daily response scans. The TSI measurements indicate that the internal lamp was stable to within ±1% during the season. The PMT currents show an abrupt jump of 3-4% occurring on 7/14/99. The reason for the change in responsivity is unknown. However, several absolute scans were run on this day and change in responsivity might have been triggered by the calibration event. The season was broken into two periods at 7/14/99 and for each of this periods a separate irradiance was assigned to the internal lamp. The change in instrument responsivity was therefore compensated for by the calibration. By comparing readings of the TSI sensor during solar measurements with concurrent measurements of spectral irradiance, which had been weighted with the spectral responsivity curve of the TSI sensor, it was verified that the change in responsivity did not have an impact on solar data. The ratio of both independent measurements was not significantly different before and after July 14.

Figure 5.6.3 also shows the time series of monochromator temperature. Usually, the temperature is stable to within tenths of a degree. Between 7/1/99 and 7/8/99, however, the temperature is high by 2 °C during scans of the internal irradiance reference and by as much as 4.5 °C during solar measurments. For unknown reasons, the temperature stabilization of the instrument did not work during this period. The rise in

temperature led to greater scatter in the PMT currents. In addition, a detailed analysis of the wavelength position shows that, during the affected period, there is a diurnal cycle in the wavelength offset on the order of ±0.1 nm (see Section 5.6.3). The uncertainty of solar measurements during this periods is increased by about ±2% in the UV-A and visible, and approximately ±5% in the short-wave UV-B.

The irradiance assigned to the internal lamp in Period 1 was calculated by analyzing 25 calibrations with the site irradiance standards carried out during this period. From each of these calibrations, irradiance values for the internal lamp were calculated and the mean-irradiance for this period was derived by averaging over the individual calibration functions, according to the procedure outlined in Section 4.2.1.2. The ratio of the standard deviation and average mean-irradiance, both calculated from the 25 calibrations, is a useful tool for estimating the variability of the calibrations for this period. As shown in Figure 5.6.4, the standard deviation is approximately 1.5% of the average. Thus calibrations during Period 1 are consistent to the ±1.5% (±1σ) level. The same procedure was also applied to Period 2, during which 12 calibrations were performed. The standard-deviation-to-average ratio for this period is also shown in Figure 5.6.4.

Figure 5.6.5 shows the ratio of the irradiance assigned to the internal lamp in Period 1 and Period 2. As can be seen, the irradiance of Period 2 is about 1-4% lower than the irradiance assignment of Period 1.

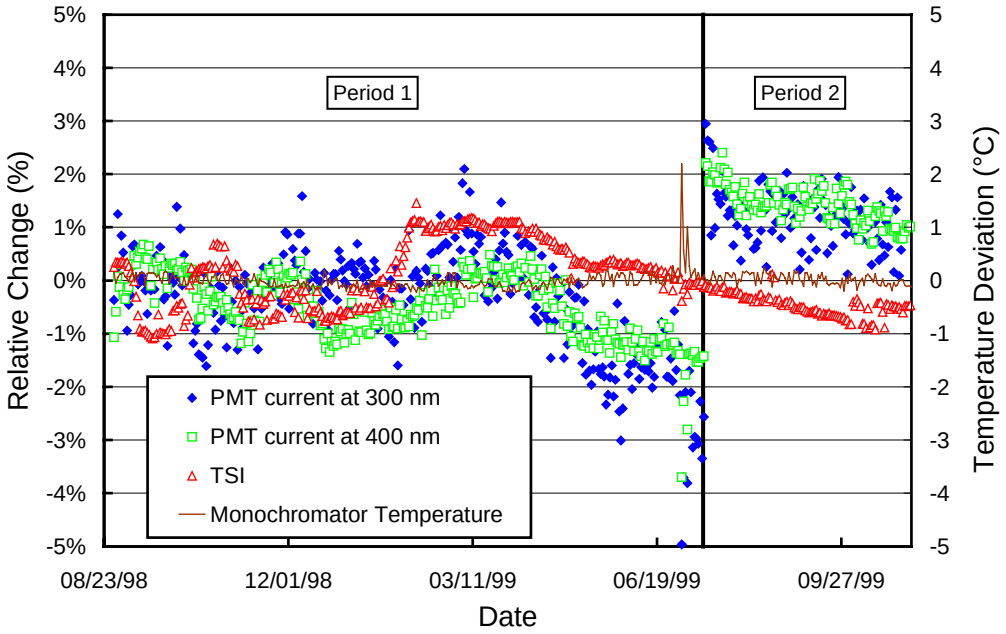


**Figure 5.6.3.** *Time-series of PMT current at 300 and 400 nm, TSI signal (left axis), and monochromator temperature (right axis) during measurements of the response lamp during the Barrow 1998-99 season. The data is normalized to the average of both periods.*

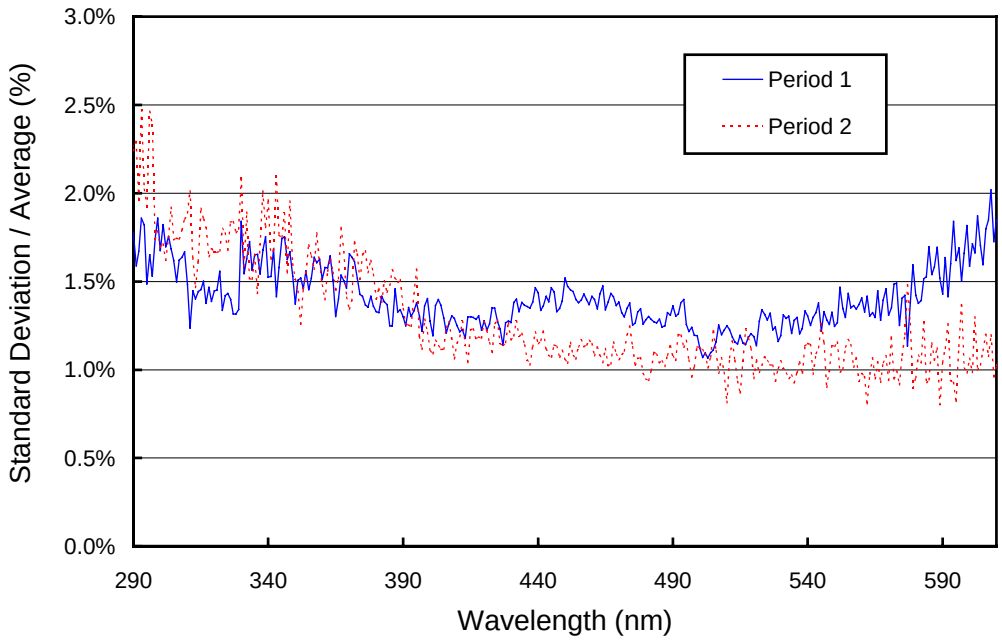


**Figure 5.6.4.** *Ratio of standard deviation and average calculated from the absolute calibration scans of Periods 1 and 2.*

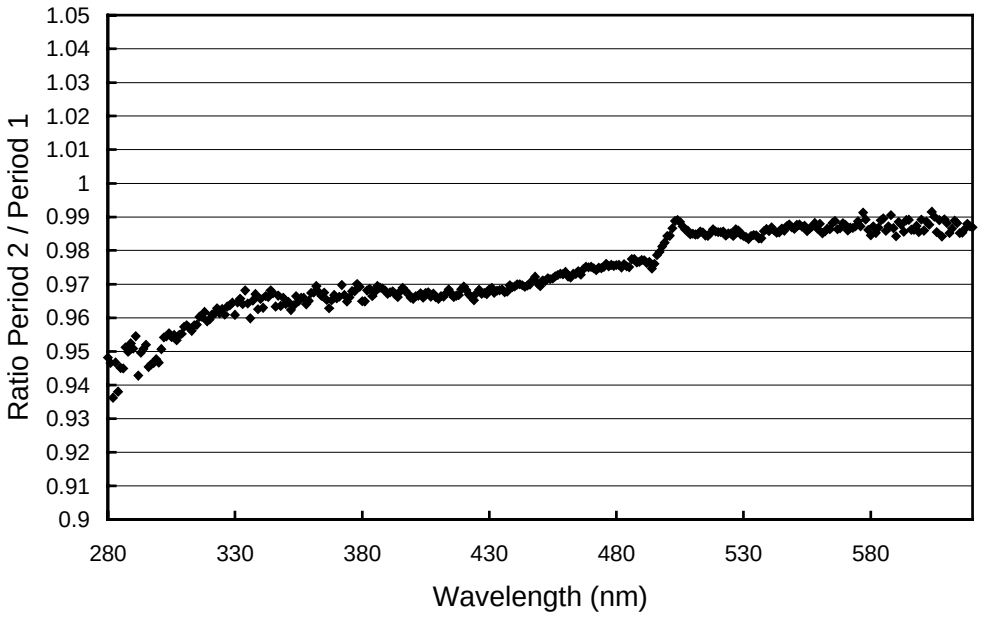


**Figure 5.6.5.** *Ratio of irradiance assigned to the internal reference lamp of Period 2 to Period 1.*

### 5.6.3. Wavelength Calibration

Wavelength stability of the system was monitored with the internal mercury lamp. Information from the daily wavelength scans was used to homogenize the data set by correcting day-to-day fluctuations in the wavelength offset. After this step, there may still be a deviation from the correct wavelength scale, but this bias should ideally be the same for all days. Figure 5.6.6 shows the differences in the wavelength offset of the 296.73 nm mercury line between two consecutive wavelength scans. In total, 388 scans were evaluated. For 82% of the days, the change in offset was smaller than ±0.025 nm and there was no pair of scans where the shift was larger than ±0.075 nm.

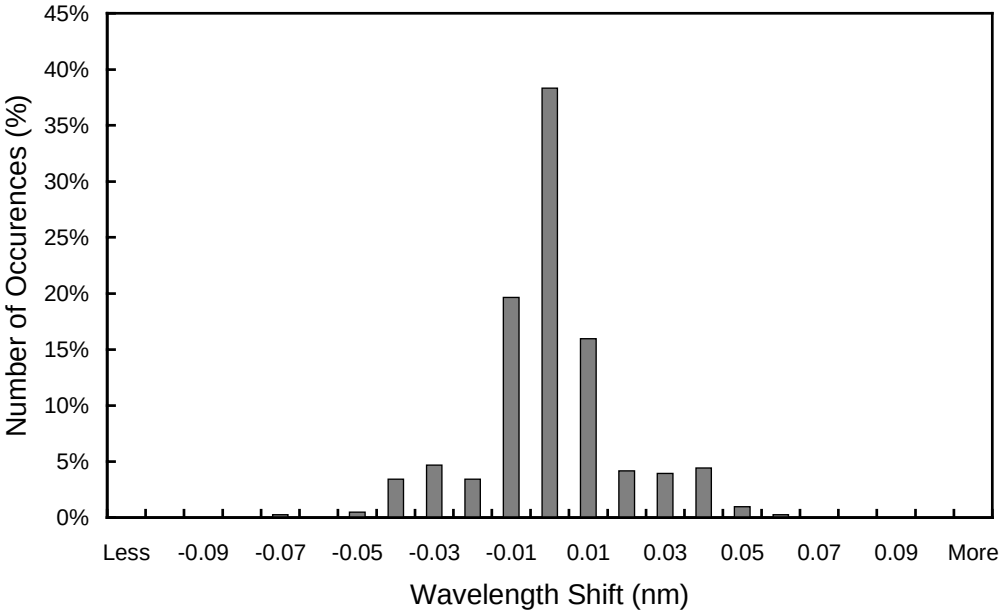


**Figure 5.6.6.** *Differences in the measured position of the 296.73 nm mercury line between consecutive wavelength scans. The x-labels give the center wavelength shift for each column. Thus the 0-nm histogram column covers the range -0.005 to +0.005 nm. "Less" means shifts smaller than –0.105 nm; "more" means shifts larger than 0.105 nm.*

After the data was corrected for day-to-day wavelength fluctuations, the wavelength-dependent bias between this homogenized data set and the correct wavelength scale was determined with the Fraunhofer-correlation method, as described in Section 4. The thick line in Figure 5.6.7 shows the resulting correction function that was applied to the Volume 8 Barrow data. The function depends upon wavelength, which is caused by non-linearities of the monochromator drive. In order to demonstrate the difference between the result of the Fraunhofer-correlation method and the method that was historically applied, Figure 5.6.7 also includes the correction function that was calculated with the "old" method, i.e., the function is based on internal wavelength scans only. The average difference between both approaches is approximately 0.14 nm. As explained in Section 4, this bias is caused by the different light paths for internal wavelength scans and solar measurements.

After the data was wavelength corrected using the shift function described above, the wavelength accuracy was confirmed again with the Fraunhofer method. The results are shown in Figure 5.6.8 for four UV wavelengths, evaluated for all noontime scans measured during the season. The residual shifts are generally smaller than ±0.05 nm. The actual wavelength uncertainty may be larger due to wavelength fluctuations of about ±0.02 nm during the day, and possible systematic errors of the Fraunhofer-correlation method (see Section 4). There is also more scatter at 310 nm, in particular between the beginning of November and end of February, because levels of solar irradiance at this wavelength are generally low at Barrow, which is

problematic for the correlation algorithm. The enhanced scatter does not mean that the wavelength uncertainty is actually larger.

Because of the increase in monochromator temperature between 7/1/99 and 7/5/99, the wavelength accuracy in this period is slightly worse. Figure 5.6.9 shows the result of the Fraunhofer correlation technique for this period. There is a diurnal pattern in the wavelength shifts of ±0.1 nm, which tracks the monochromator temperature.

Although data from the external mercury scans do not have a direct influence on the data products, they are an important part of instrument characterization. Figure 5.6.10 illustrates the difference between internal and external mercury scans collected during both site visits. The wavelength scale of the figure is the same as applied during solar measurements; the scale is based on a combination of the Fraunhofer-correlation technique and wavelength-offset determination with internal mercury scans. The peak of the external scans, which have the same light path as solar measurements, agrees well with the nominal wavelength of 296.73 nm, whereas the peak of the internal scans is shifted about 0.12 nm to shorter wavelengths. External scans have a bandwidth of about 1.04 nm FWHM, whereas the bandwidth of the internal scan is 0.80 nm. Since external scans have the same light path as solar measurements, they more realistically represent the monochromator bandpass relevant for solar scans. The scans at the start and end of the season are very consistent.

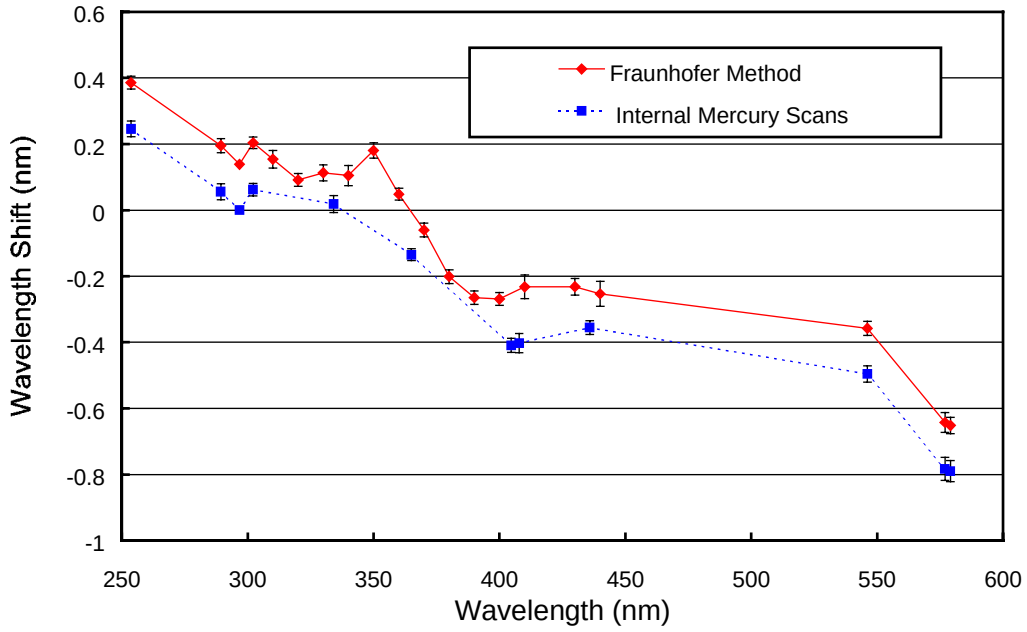


**Figure 5.6.7.** *Monochromator non-linearity for the Barrow 1998-99 season. Solid line: Correction function calculated with the Fraunhofer-correlation method, applied to correct the Barrow Volume 8 data. Thin broken line: Correction function calculated with the method that was historically applied. The mean offset difference between both methods is 0.14 nm. The error bars show the 1σ standard deviation of the wavelength shift for the season.*

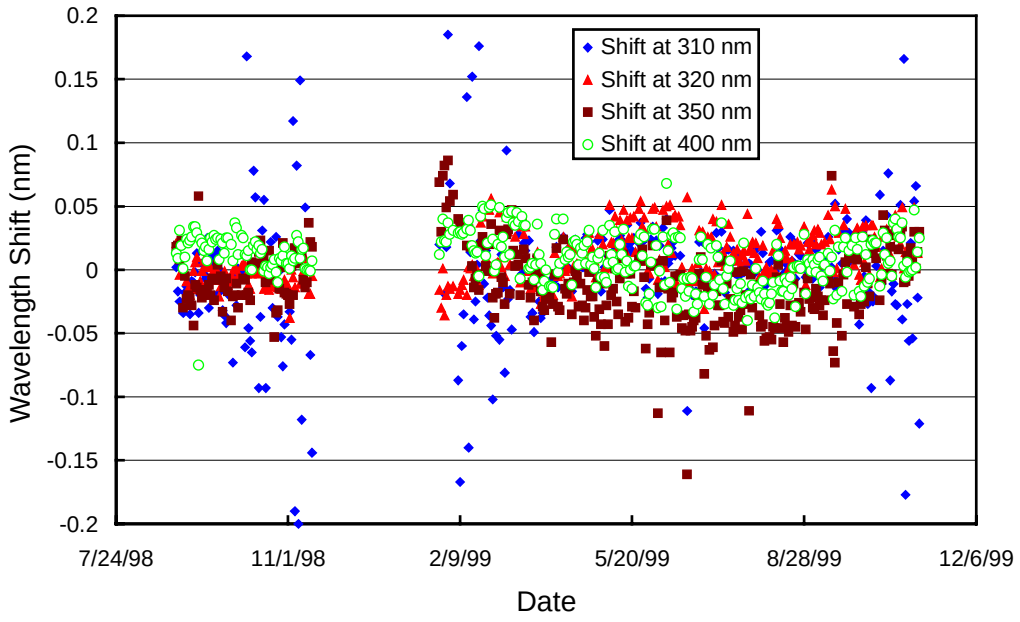


**Figure 5.6.8.** *Wavelength accuracy check of the final data at four wavelengths by means of Fraunhofer correlation. The noontime measurement has been evaluated for each day of the season when the sun was above the horizon.*

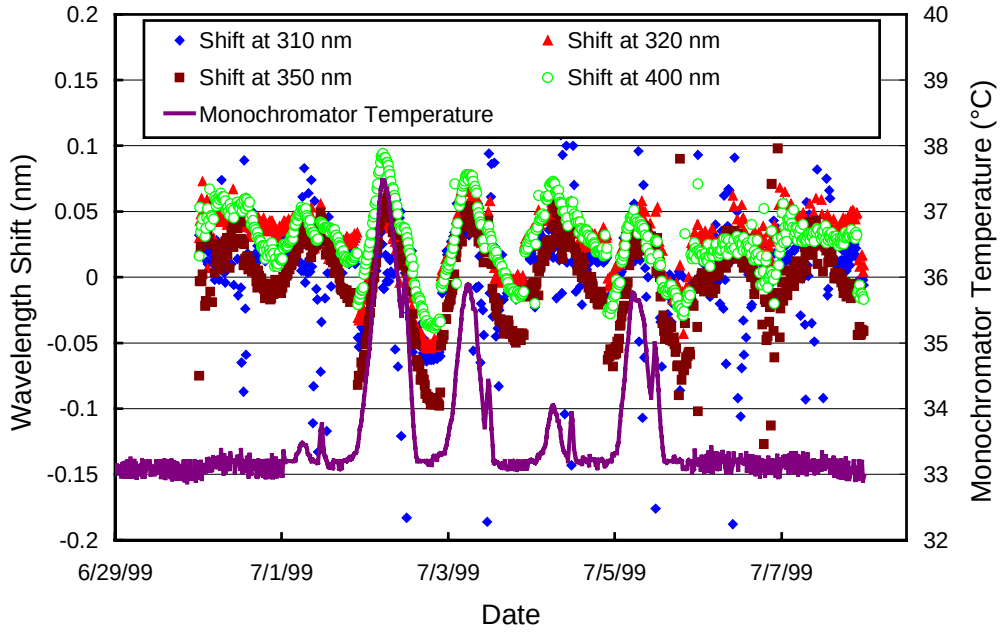


**Figure 5.6.9.** *Wavelength accuracy check of the final data at four wavelengths by means of Fraunhofer correlation between 6/30/99 and 7/8/99. Fluctuations in the wavelength position correlate with monochromator temperature.*

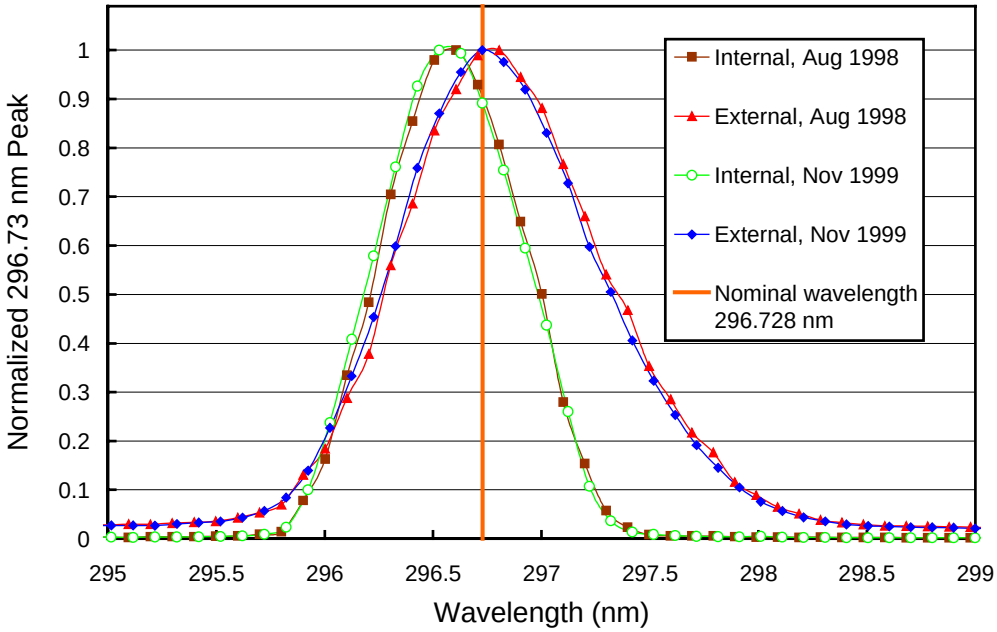


**Figure 5.6.10.** *The 296.73 mercury line as registered by the PMT from external and internal sources at the start and end of the season. The wavelength scale is the same as applied for solar measurements, i.e., it is based on a combination of internal scans and the Fraunhofer-correlation method. It is assumed that the wavelength registration of the monochromator did not shift between internal and external scans, which were close in time.*

### 5.6.4. Missing Data

A total of 22250 scans with solar zenith angles smaller than 92° were scheduled to be measured in the Barrow Volume 8 season. Of these scans, 21770 (97.8%) were found to be of useable quality and are therefore part of the published dataset. Of the missing scans, 87, 96, and 185 were superseded by absolute, wavelength, and response scans, respectively. Since Barrow has 24 hours of sunlight per day during the daylight season, the loss of these data scans cannot be avoided. Finally, a total of 112 scans were lost for various other reasons. Among them, 15 scans were lost during computer configuration, mostly on 10/4/98. During change of storage media or due to problems with the peripheral hard disk drive 10 scans were lost. During four instances a data scan took longer than 15 minutes and the following data scan was not started. At least 12 scans were not started due to operator intervention. Thirty two scans in March and April 1999 (22 on 3/20/99) were not stored correctly on the hard disk drive, although they had been measured. A total of 22515 scans are listed in the published databases, including 743 scans with solar zenith angles between 92° and 95°.